Urania
Jurnal Ilmiah Daur Bahan Bakar Nuklir

Beranda jurnal: https://ejournal.brin.go.id/urania/

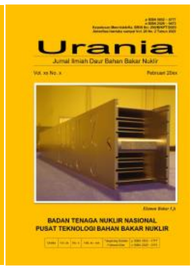

INFLUENCE OF Mo AND Nb CONTENT ON THE MECHANICAL AND CORROSION PROPERTIES OF AlCrMoNbZr HIGH-ENTROPY ALLOYS FOR NUCLEAR FUEL CLADDING

Heri Hardiyanti[1,2], Marzuki Naibaho[1,3], Budhy Kurniawan[1], Jan Setiawan[3,4], Masno Ginting[3], Andon Isnani[2], Januar Widakdo[1]
[1]Department of Physics, Faculty of Mathematics and Natural Sciences, Universitas Indonesia
Depok, Jawa Barat, Indonesia 16424
[2]Research Center for Nuclear Materials and Radioactive Waste Technology – BRIN
KST B.J. Habibie, Serpong, Tangerang Selatan, Banten, Indonesia 15314
[3]Research Center for Advanced Materials – BRIN
KST B.J. Habibie, Serpong, Tangerang Selatan, Banten, Indonesia 15314
[4]Department of Electrical Engineering, Universitas Pamulang
Jl. Raya Puspiptek, Tangerang Selatan, Banten, Indonesia, 15310
Email: ando001@brin.go.id; Januar.widakdo@ui.ac.id

(Submitted: 16–04–2025, Revised: 20–05–2025, Accepted: 23–05–2025)

ABSTRACT

INFLUENCE OF Mo AND Nb CONTENT ON THE MECHANICAL AND CORROSION PROPERTIES OF AlCrMoNbZr HIGH-ENTROPY ALLOYS FOR NUCLEAR FUEL CLADDING. The effect of varying Mo and Nb content in AlCrMo5%NbZr and AlCrMoNb5%Zr on their mechanical and corrosion properties has been investigated. X-ray diffraction (XRD) analysis revealed the presence of cubic and hexagonal crystal structure, with AlCrMoNb5%Zr exhibiting a higher concentration of hexagonal structures, contributing to improved hardness and corrosion resistance. Scanning electron microscopy (SEM) and energy-dispersive spectroscopy (EDS) confirmed a dendritic morphology with uniform elemental distribution for both samples. Vickers hardness and the corrosion testing shows the AlCrMoNb5%Zr has superior hardness and significantly lower corrosion rate compared to AlCrMo5%NbZr, respectively. These findings suggest that less amount of Nb content enhances mechanical and corrosion properties, making AlCrMoNb5%Zr a potential material for nuclear reactor applications, mainly as fuel cladding material.

Keywords: High Entropy Alloys (HEAs), AlCrMoNbZr, crystal structure, microstructure, hardness, corrosion.

INTRODUCTION

Nuclear energy plays a significant role in meeting global energy demands. Since the 1970s, it has proven to be reliable, environmentally friendly, clean, cost-effective, and a widely utilized energy source [1]. Given the prolonged contact of cladding with water, the material must possess excellent corrosion resistance to prevent degradation, which could lead to nuclear fuel particle release and radiation leaks [2], [3], [4]. as in the Fukushima incident in 2011 [5].

The nuclear community has since recognized the need to enhance the existing high-temperature steam corrosion resistance of Zr-based cladding alloys under beyond-design-basis accident scenarios in light water reactors (LWRs) [6], [7], [8]. In 2014, the Accident Tolerant Fuel (ATF) strategy was proposed to improve cladding corrosion resistance in Loss-of-Coolant Accident (LOCA) scenarios [9], [10].

Thus, the development of suitable alloys for atomic fuel cladding is essential. One promising candidate material is high entropy alloys (HEAs). HEAs have superior microstructure and unique properties, such as high hardness and excellent corrosion resistance. HEAs typically consist of five or more principal elements in equimolar or near-equimolar ratios, with each element's atomic concentration between 5% and 35%.

Compared to Zr alloys, HEAs have the potential for nuclear fuel cladding as shown in comparable corrosion rate with Zr 0.0932 mpy, Zirlo Mo 0.5903 mpy, Zry-2 0.0061 mpy, Zry-4 0.0071 mpy [Maman et,all.] [11]. The research of HEA for nuclear fuel cladding has been investigated with several element combinations as shown in Table 1.

In this study, we aim to synthesize AlCrMoNbZr high-entropy alloys with different Mo and Nb contents, specifically AlCrMo5%NbZr and AlCrMoNb$_5$%Zr, using the arc melting method with a single-electrode arc furnace. The alloy composition was calculated based on each element's relative atomic mass (Ar) and molar quantities. This research aims to identify the phases, microstructures, mechanical properties, and corrosion rates in a wt% NaCl solution of AlCrMo5%NbZr and AlCrMoNb5%Zr HEAs sample.

Table 1. Previous research in HEA alloys used as structural or cladding materials for nuclear fuel applications.

No	Composition (HEA)	Reference
1	AlCrCuFeNb	[12]
2	AlCrCuFeNb0.3	[12]
3	AlCrCuFeNb0.5	[12]
4	AlCrCuFeNb0.7	[12]
5	MoNbCrVTi	[13]
6	MoNbCrZrTi	[13]
7	AlCrFeNiMo	[14]
8	AlCrFeNiZr	[14]

METHODOLOGY.

a. Fabrication of AlCrMo5%NbZr and AlCrMoNb5%Zr HEAs

HEAs AlCrMo5%NbZr and AlCrMoNb5%Zr with a target weight of 10 g were fabricated using a vacuum arc melting furnace under a pure argon atmosphere. All elements used had a purity of more than 99.9%. To ensure homogeneous elemental distribution, the ingots were remelted more than five times, flipping the ingot after each melting process using a vacuum arc melting. The elemental composition of the AlCrMo5%NbZr and AlCrMoNb5%Zr alloys studied is presented in Table 2.

Figure 1 illustrates the resulting ingots of HEAs AlCrMo5%NbZr and AlCrMoNb5%Zr. The specimens were button-shaped, with a diameter of approximately 10.5 mm and a height of 7 mm. After melting, they were sectioned into smaller parts using a Struers Secotom-20 diamond cutter and further processed into samples for various testing purposes.

Table 2. Atomic percent and weight percent of the elements of the HEA sample.

HEAs	Element	at.%	wt.%
AlCrMo5%NbZr	Al	23.75	9.52
	Cr	23.75	18.35
	Mo	5.00	7.13
	Nb	23.75	32.80
	Zr	23.75	32.20
AlCrMoNb5%Zr	Al	23.75	9.44
	Cr	23.75	18.20
	Mo	23.75	33.58
	Nb	5.00	6.85
	Zr	23.75	31.93

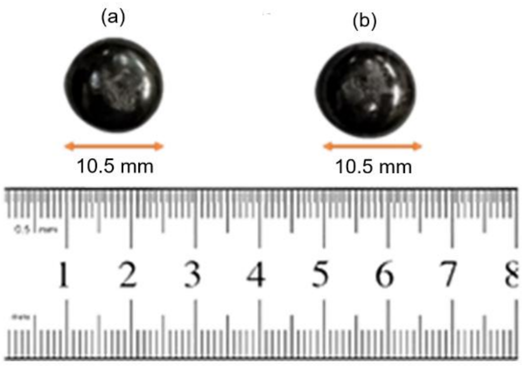

Figure 1. Ingot HEAs (a) AlCrMo5%NbZr dan AlCrMoNb5%Zr

b. Characterization

Phase analysis of the AlCrMo5%NbZr and AlCrMoNb5%Zr samples was performed using a Panalytical Empyrean Diffractometer with a cobalt anode X-ray source. The microstructure of the HEAs was analyzed using a Phenom Paros SEM-EDS to observe microstructural details and quantify elemental composition by weight. Hardness testing was conducted three times using a Vickers Hardness Tester (LM800T) with an indentation time of ten seconds in the seven different points. The corrosion rates of the HEAs samples, AlCrMo5%NbZr and AlCrMoNb5%Zr, were measured using a Gamry Reference 3000 Potentiostat with a three-electrode system. A platinum electrode served as the auxiliary electrode, Ag/AgCl was used as the reference electrode, and the sample functioned as the working electrode. The analysis was conducted through potentiodynamic polarization, starting from an initial potential of -0.3 V relative to the open circuit potential (Eoc) to a final potential of 0.3 V relative to Eoc, with a scanning rate of 0.005 V/s in a 3wt% NaCl solution. The all surface area of samples after cutting was measured with the average dimension is 0.5×1 cm.

RESULTS AND DISCUSSION

a. Phase Analysis of AlCrMo5%NbZr and AlCrMoNb5%Zr HEAs Samples

Figure 2 illustrates the X-ray diffraction (XRD) patterns of the HEAs samples AlCrMo5%NbZr and AlCrMoNb5%Zr. From the analysis of the AlCrMo5%NbZr sample, the identified phases include Al0.2Nb0.8 (ICSD 98-010-7858), Nb1Zr1 (ICSD 98-064-5570), and Mo0.875Zr0.125, which exhibit cubic crystal structures. Al2Zr1 with a hexagonal crystal structure (ICSD 98-005-5594) was also observed. These results indicate that the reduction in molybdenum (Mo) content, attributed to its large atomic radius, induces lattice distortion and promotes solid solution strengthening. This phenomenon leads to a gradual increase in the lattice constant of the cubic structure, as previously demonstrated in studies on HEAs [1]. Despite this, the hexagonal structure within the sample signifies its resilience under compositional changes.

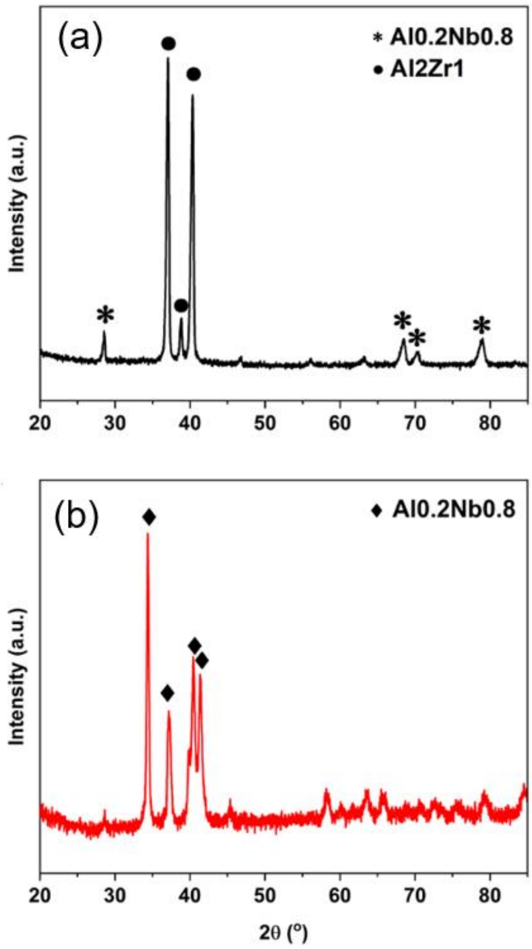

Figure 2. XRD patterns of the AlCrMo5%NbZr (a) and AlCrMoNb5%Zr (b)

In the AlCrMo5%NbZr HEA, the primary phase formed is Al2Zr1 (hexagonal, 67%), supported by the Al0.2Nb0.8 (cubic, 33%) phase, resulting in a dominant hexagonal structure. In contrast, the AlCrMoNb5%Zr HEA predominantly forms the $Al_1Cr_1Zr_1$ phase (hexagonal, 100%), exhibiting a fully hexagonal structure. The phase structure formed in HEAs is strongly influenced by several factors, one of which is atomic size. HEAs consist of multiple elements with varying atomic radii. When the atomic size difference is relatively small, the alloy tends to form a solid solution typically with a cubic structure. However, if the size difference is too large, it may lead to the formation of intermetallic phases such as hexagonal structures [15][16].

The AlCrMoNb5%Zr sample exhibited the Al1Cr1Zr1 phase, corresponding to a hexagonal crystal structure per ICSD 98-060-6876. The inclusion of niobium (Nb) in the structure enhances the "cocktail effect," enriching elemental interactions and providing new dimensions for mechanical property optimization [1]. The gradual dominance of the hexagonal lattice constant in this sample reflects its structural stability and reinforces its suitability for high-performance applications. The identified phases and their respective properties are summarized in Table 2.

Consistent with previous studies by Wang et al. [17] And Salam R. et al. [18] The presence of Al_2Zr in high concentrations within the AlCrMo5%NbZr sample demonstrates its potential for applications demanding high thermal stability. Hexagonal crystal structures, such as those formed by Al_2Zr, are renowned for their temperature resistance, making this sample an excellent candidate for high-temperature environments.

Table 1. Phases of HEA AlCrMo5%NbZr and AlCrMoNb5%Zr.

HEA	Phases	Space Group	Crystal system	Weight (%)
AlCrMo5%NbZr	Al0.2Nb0.8 ICSD 98-010-7858	Im-3 m	Cubic	33
	Al2Zr1 ICSD 98-005-5594	P 63/m m c	Hexagonal	67
AlCrMoNb5%Zr	Al1Cr1Zr1 ICSD 98-060-6876	P 63/m m c	Hexagonal	100

Moreover, the AlCrMoNb5%Zr sample, dominated by the Al1Cr1Zr1 phase, is particularly noteworthy for its enhanced corrosion resistance and high mechanical strength. This can be attributed to the uniform distribution of Nb and the hexagonal lattice structure, which contribute to developing materials with superior anti-corrosion behavior and mechanical performance. Such properties expand the potential application scope of this alloy, particularly in environments where both thermal stability and corrosion resistance are critical.

b. Microstructural Analysis of AlCrMo5%NbZr and AlCrMoNb5%Zr HEAs Samples

The microstructures of the HEA samples AlCrMo5%NbZr and AlCrMoNb5%Zr were analyzed using scanning electron microscopy and energy-dispersive spectroscopy (SEM-EDS) at magnifications of 1000x, 2500x, and 5000x (Figure 3). The results reveal that both samples exhibit a dendritic morphology, with the dendritic structure comprising primary and secondary or tertiary branches extending from these main branches. This morphology results from directional solidification during cooling, driven by temperature and concentration gradients.

The formation of dendritic structures in HEAs can also be attributed to high-melting-point elements, such as Mo, Nb, and Zr, which influence the solidification process and contribute to structural evolution. As shown in Figure 3, the AlCrMo5%NbZr sample exhibits a more prominent dendritic structure than the AlCrMoNb5%Zr sample. This difference may be due to variations in Nb and Mo concentrations, which influence the alloy's crystallization kinetics and solidification pathways. Dendritic structures in metallic systems, particularly HEAs, enhance mechanical strength and hardness due to their inherent anisotropy and hierarchical morphology. The more pronounced dendritic structure observed in the AlCrMo5%NbZr sample may result in localized strengthening, contributing to its improved mechanical stability. However, the slightly reduced dendritic structure in the AlCrMoNb5%Zr sample suggests a more uniform elemental distribution, which can enhance overall mechanical and thermal stability while balancing hardness with ductility.

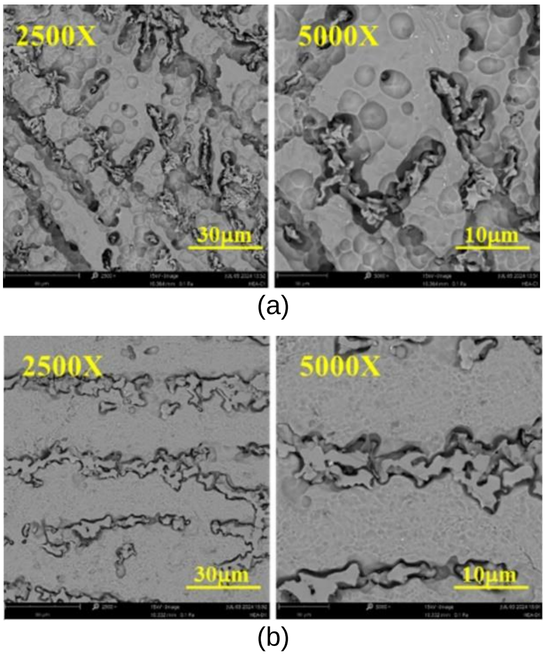

Figure 3. Microstructure of SEM results of HEAs samples (a) AlCrMo5%NbZr and (b) AlCrMoNb5%Zr.

This aligns with findings from previous studies on HEAs, where dendritic morphologies correlate with improved load-bearing capacity and resistance to deformation under stress. Furthermore, the elemental composition, particularly the inclusion of Nb, plays a critical role in the observed structural features. Nb contributes to the "cocktail effect," introducing synergistic interactions between constituent elements, which can further optimize mechanical properties [1][2].

The microstructural analysis highlights the importance of composition and processing conditions in tailoring the properties of HEAs. The pronounced dendritic structure in AlCrMo5%NbZr provides insights into its solidification behavior, while the reduced dendritic structure in AlCrMoNb5%Zr demonstrates the role of compositional adjustments in influencing microstructural refinement. These findings emphasize the potential of these HEAs for applications requiring high strength and thermal stability.

Figure 4 (a) and (b) present the SEM-EDS characterization results for the HEAs samples AlCrMo5%NbZr and AlCrMoNb5%Zr, revealing a dendritic morphology in both cases.

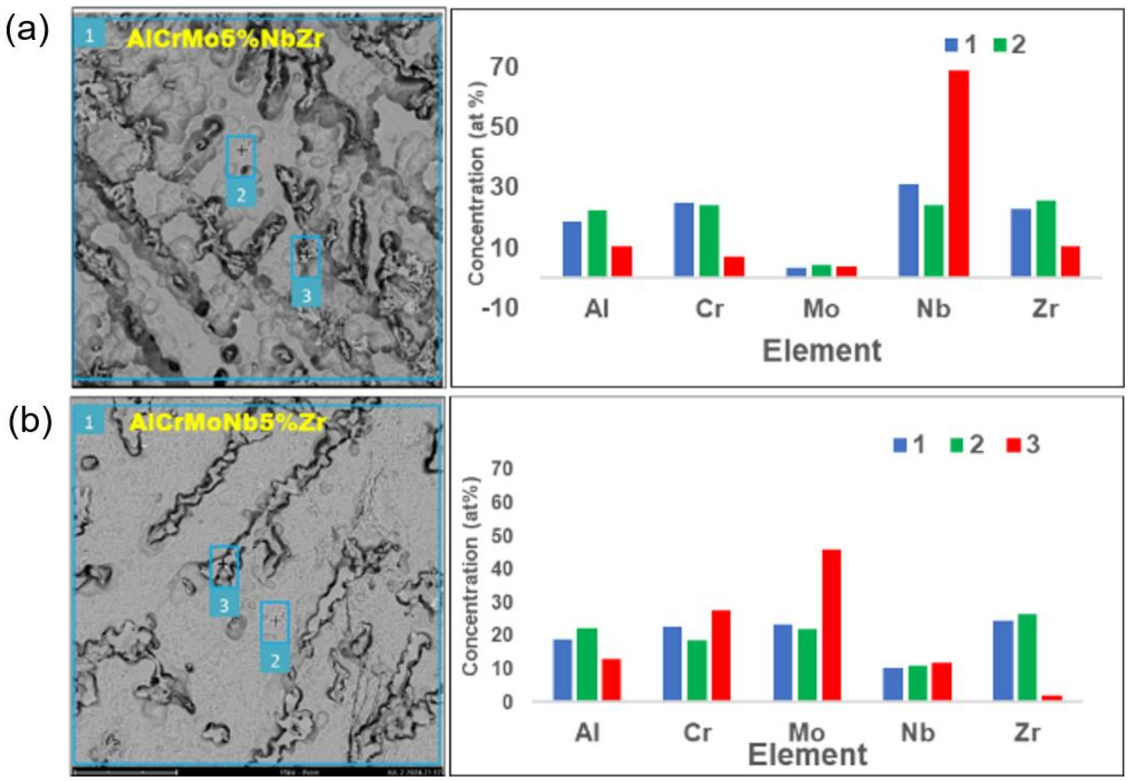

Figure 4. SEM-EDS analysis of HEA surfaces (a) AlCrMo5%NbZr and (b) AlCrMoNb5%Zr.

The dendritic microstructures in Figure 4 consist of primary and secondary branches, indicating the solidification pathway during alloy formation. The distribution of key alloying elements, such as Mo, Nb, Zr, Cr, and Al, is relatively uniform across the dendritic and interdendritic regions, as evident in the EDS results (Figure 4 (a) and (b)). The near-homogeneous elemental distribution suggests adequate mixing during the arc-melting process, a critical factor in stabilizing the high-entropy alloy. Notably, the presence of Mo and Nb, both elements with high melting points significantly influences the solidification kinetics and dendritic growth. These elements are more concentrated in specific regions,

As shown in Figure 4 (a), the AlCrMo5%NbZr sample exhibits a more prominent dendritic morphology compared to the AlCrMoNb5%Zr sample in Figure 4 (b). Substituting Mo with Nb appears to refine the microstructure by reducing the size of the dendritic branches. This is supported by the more homogeneous elemental distribution in AlCrMoNb5%Zr, as indicated by the reduced intensity fluctuations in the EDS results (Figure 4 (b)). Nb's higher concentration in AlCrMoNb5%Zr enhances the "cocktail effect," where the interactions between diverse elements result in lattice distortions and solid solution strengthening. The substitution effect may also reduce lattice mismatch, contributing to microstructural stability and thermal resistance.

The microstructural homogeneity and refined dendritic morphology observed in AlCrMoNb5%Zr are expected to improve its mechanical and corrosion resistance properties. While contributing to hardness, Mo-rich phases may introduce microsegregation, which could lead to localized electrochemical differences. In contrast, the uniform distribution of Nb in AlCrMoNb5%Zr minimizes such effects, potentially enhancing its overall performance in corrosive environments. These findings align with previous studies, such as those by Wang et al. [1], which emphasize the role of homogeneous microstructures in improving mechanical stability and corrosion resistance in HEAs. The dendritic morphology, combined with the elemental homogeneity, makes AlCrMoNb5%Zr a promising candidate for applications requiring high thermal and corrosion resistance, particularly in nuclear fuel cladding materials.

Figures 5 (a) and (b) present the elemental mapping and semi-quantitative EDS analysis for AlCrMo5%NbZr and AlCrMoNb5%Zr, respectively. The results indicate that the alloying elements—Al, Cr, Mo, Nb, and Zr—are uniformly distributed across the surface of both alloys.

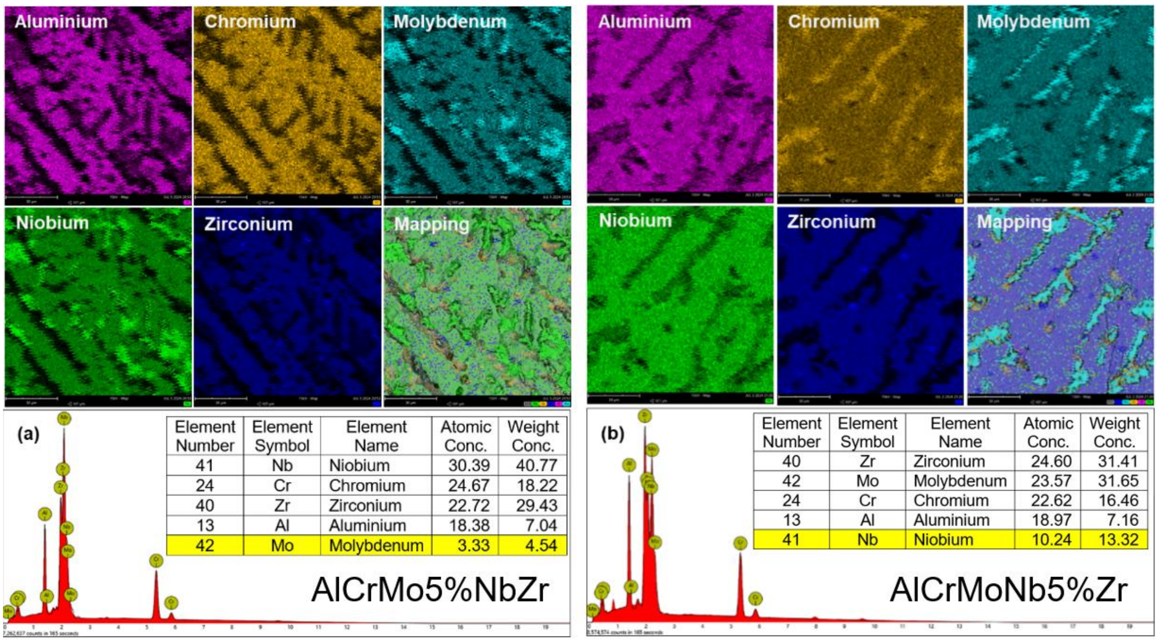

(a) (b)

Figure 5. SEM-EDS analysis of HEA samples AlCrMo5%NbZr (a), and AlCrMoNb5%Zr (b).

This homogeneous distribution is a hallmark of high-entropy alloys (HEAs), achieved due to the high-entropy mixing during the synthesis process. In the AlCrMo5%NbZr sample (Figure 5 (a)), the elemental mapping highlights Mo and Nb as the dominant elements, with Nb showing the highest atomic concentration at 30.49 at%. Similarly, for the AlCrMoNb5%Zr sample (Figure 5 (b)), the dominant elements remain Nb and Mo, with Nb again taking precedence at 31.40 at%. This result is consistent with the alloy design, emphasizing refractory elements like Mo and Nb for enhanced mechanical properties and thermal stability.

The dominance of Nb and Mo in both samples significantly influences the material properties. Nb is well-known for enhancing solid solution strengthening and stabilizing the microstructure due to its high melting point and sizeable atomic radius. Additionally, the high concentration of Mo contributes to hardness and wear resistance, as it typically forms strong metallic bonds and stable solid solutions. The uniformity observed in the elemental distribution across the alloys, as demonstrated in the mapping images, minimizes potential regions of segregation. Such uniformity is crucial in maintaining isotropic mechanical properties and ensuring consistent performance across various applications, particularly under high-temperature and corrosive environments.

Comparing Figures 5 (a) and (b), both samples exhibit a similar trend in elemental distribution. However, the substitution of Nb with Mo in AlCrMoNb5%Zr results in a slight variation in weight concentration, with Zr showing a higher presence (31.65 wt%) compared to AlCrMo5%NbZr (22.77 wt%). This substitution alters the overall atomic arrangement and may improve thermal stability and mechanical strength in AlCrMoNb5%Zr. The nearly identical mapping results of Cr and Al further demonstrate the role of these elements in forming a stable base for the alloy system. On the other hand, Zr plays a dual role: as a solute in the solid solution and a promoter of secondary phase formation, enhancing both ductility and thermal properties.

The semi-quantitative EDS analysis and elemental mapping results indicate that these HEAs exhibit a well-balanced composition with uniform elemental distribution, which is critical for applications requiring high structural integrity. The dominance of Nb and Mo in these alloys aligns with findings by Wang et al. [1] and Salam R. et al. [2], which emphasize the importance of refractory metals in improving mechanical and thermal properties.

c. Hardness Properties of AlCrMo5%NbZr and AlCrMoNb5%Zr HEAs Samples

Their microstructural features and elemental composition significantly influence high-entropy alloys' mechanical performance (HEAs). The hardness analysis of the HEA samples, as depicted in Figure 6, provides critical insights into the effects of varying Nb and Mo content on mechanical properties. The Vickers hardness test, conducted under a load of 100 gF with an indentation time of 10–15 seconds, yielded hardness values of 717 HV for AlCrMo5%NbZr and 742 HV for AlCrMoNb5%Zr.

The observed increase in hardness with the reduction in Nb content can be attributed to the intrinsic properties of Nb and its influence on the crystal structure. Nb, a refractory element with a high melting point and a body-centered cubic (BCC) crystal structure, promotes solid solution strengthening by contributing to lattice distortion. The substitution of Nb with a higher percentage of Mo in AlCrMoNb5%Zr intensifies this strengthening mechanism. Mo, also a refractory element with a BCC structure, enhances the "cocktail effect," which refers to the synergistic interaction of diverse atomic sizes, electronegativities, and valences within the alloy matrix.

As described in earlier studies [1], the cocktail effect arises from the unique combination of alloying elements in HEAs. Elements such as Nb and Mo introduce complex interactions among atoms, leading to lattice distortion and strengthening. In the case of AlCrMoNb5%Zr, the higher Mo content enhances the hardness due to its ability to form stronger metallic bonds than Nb. This results in a more resistant alloy matrix capable of withstanding higher indentation loads during the Vickers hardness test.

The difference in hardness values (742 HV for AlCrMoNb5%Zr vs. 717 HV for AlCrMo5%NbZr) highlights the critical role of alloy composition in tailoring mechanical properties. The higher hardness of AlCrMoNb5%Zr suggests that substituting Nb with Mo increases the alloy's resistance to plastic deformation. This aligns with similar studies, which emphasize the importance of refractory elements like Mo in enhancing the HEAs mechanical performance.

The results underscore the significance of carefully balancing refractory elements in HEAs to achieve desired mechanical properties. While Nb contributes to strengthening solid solutions and thermal stability, substituting it with Mo introduces additional lattice distortion, further enhancing hardness. This trade-off between Nb and Mo content offers a pathway for optimizing HEAs compositions for specific applications, such as wear-resistant coatings or high-strength structural materials.

The hardness analysis demonstrates that AlCrMoNb5%Zr has superior mechanical properties compared to AlCrMo5%NbZr, which are attributable to the combined effects of Mo and the cocktail effect. The findings validate the effectiveness of compositional tuning in HEAs for achieving enhanced hardness and offer valuable insights for future alloy design and application.

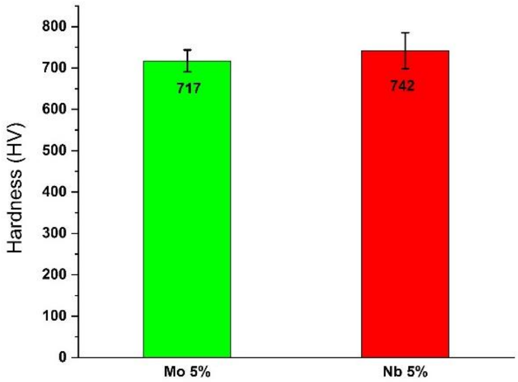

Figure 6. The hardness values of the HEAs samples AlCrMo5%NbZr (a); and AlCrMoNb5%Zr (b).

d. Corrosion Analysis of AlCrMo5%NbZr and AlCrMoNb5%Zr HEAs Samples

Corrosion resistance is a critical parameter in evaluating the suitability of high-entropy alloys (HEAs) for extreme environments, particularly in applications such as nuclear reactors. The corrosion behavior of the HEA samples, AlCrMo5%NbZr and AlCrMoNb5%Zr, was assessed through potentiodynamic polarization testing in a 3 wt% NaCl solution, as illustrated in Figure 7. This simulated the aggressive environment encountered during potential reactor accidents[19].

The polarization curves in Figure 7 reveal distinct differences in the corrosion resistance of the two HEA samples. The corrosion potential (Ecorr) and current density (Icorr) values were derived using extrapolation methods, and the corresponding corrosion rates were calculated. AlCrMoNb5%Zr exhibited a significantly lower corrosion rate of 0.24 mpy compared to 0.55 mpy for AlCrMo5%NbZr (see Table 3). These results align with the findings of Zhiming Shi et al. [20], where a higher Ecorr and a lower Icorr indicate improved corrosion resistance.

The superior corrosion resistance of AlCrMoNb5%Zr can be attributed to its optimized elemental composition and microstructural characteristics. This HEA's reduction in Nb content influences its corrosion behavior by altering the microstructural distribution. Specifically, a higher concentration of the hexagonal close-packed (HCP) structure in AlCrMoNb5%Zr results in a more uniform distribution of alloying elements. This uniformity minimizes localized corrosion and enhances the alloy's resistance to aggressive chemical attacks.

Additionally, the decreased dendritic formation in AlCrMoNb5%Zr contributes to its enhanced performance. Dendritic microstructures often exhibit compositional segregation, creating potential sites for preferential corrosion. The reduced dendritic size in AlCrMoNb5%Zr and uniform elemental distribution eliminate such vulnerabilities, leading to superior anti-corrosion behavior.

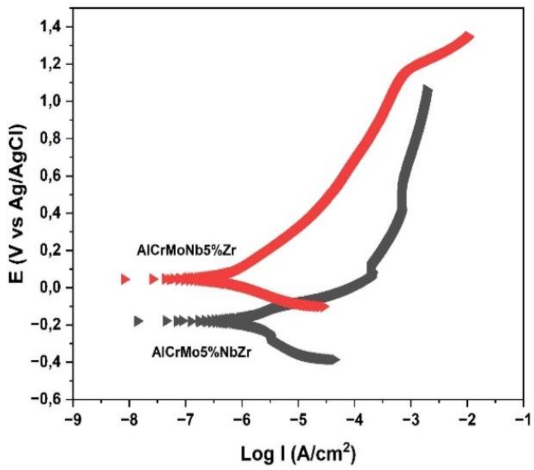

Figure 7. Polarisation curve of HEA AlCrMo5%NbZr and AlCrMoNb5%Zr with 3% NaCl solution.

Table 3. The corrosion rate of the HEA sample with 3% NaCl solution.

Sample HEA	Icorr ($\mu A/cm^2$)	Ecorr (mV)	Corrosion rate (mpy)
AlCrMo5%NbZr	1.45	-179.0	0.55
AlCrMoNb5%Zr	0.69	-44.6	0.24

In contrast, the higher Nb content in AlCrMo5%NbZr results in a more pronounced dendritic microstructure, as highlighted in previous sections. This morphology promotes elemental segregation, particularly at grain boundaries, which are active sites for corrosion initiation. The higher corrosion rate of 0.55 mpy for AlCrMo5%NbZr underscores the adverse impact of this microstructural characteristic on its corrosion resistance.

The findings highlight the potential of AlCrMoNb5%Zr as a candidate material for applications in nuclear fuel cladding, where both mechanical integrity and corrosion resistance are critical. Its superior hardness, thermal stability, and low corrosion rate make it a promising option for withstanding extreme reactor conditions. AlCrMoNb5%Zr achieves a balance of properties that address the dual challenges of corrosion resistance and mechanical performance by adding small amount Nb content and optimizing the alloy composition.

The corrosion rate analysis demonstrates that the reduction in Nb content and the resulting microstructural modifications significantly enhance the anti-corrosion properties of AlCrMoNb5%Zr. These improvements are driven by a uniform elemental distribution, reduced dendritic formation, and the predominance of the HCP structure. The results establish AlCrMoNb5%Zr as a strong candidate for further exploration and application in nuclear reactor environments, particularly as a material for fuel cladding

CONCLUSIONS

This study systematically analyzed the microstructural, mechanical, and corrosion properties of AlCrMo5%NbZr and AlCrMoNb5%Zr HEAs. The AlCrMo5%NbZr HEA has the Nb_1Zr_1 as the primary phase, with the cubic structure. In contrast, the AlCrNoNb5%Zr HEA predominantly forms the $Al_1Cr_1Zr_1$ phase with the hexagonal structure. The small content of the Nb as in AlcrMoNb5%Zr HEA show significantly influenced its properties, leading to a more uniform microstructure with reduced dendritic formation. This alloy exhibited superior hardness (742 HV) and enhanced corrosion resistance, with a corrosion rate of 0.24 mpy compared to 0.55 mpy for AlCrMo5%NbZr. These improvements were attributed to the uniform elemental distribution, dominance of the hexagonal structure, and reduced segregation. The combination of high hardness, excellent corrosion resistance, and thermal stability makes AlCrMoNb5%Zr a promising candidate for applications in extreme environments, such as nuclear fuel cladding. The further investigation such as tested under actual nuclear reactor conditions, tensile and impact testing, and thermal performance evaluations were needed to tested the capability of HEAs in Nuclear fuel cladding aplication.

ACKNOWLEDGEMENTS

The authors would like to express their gratitude to the Organisasi Riset Tenaga Nuklir, Badan Riset dan Inovasi Nasional (BRIN) for their support and funding under the Keputusan Kepala Organisasi Riset Tenaga Nuklir, Badan Riset dan Inovasi Nasional No. 24/III.2/HK/2023 regarding the research proposal activities within the Nuclear Technology Innovation Program for the year 2024. This support has been instrumental in facilitating the successful completion of this research. The authors also acknowledge the contributions of colleagues and collaborators who provided valuable insights and assistance throughout the research process.

AUTHOR CONTRIBUTIONS

Heri Hardiyanti: Conceptualization, Writing – original draft, Writing – review & editing, Investigation, Formal analysis, **Marzuki Naibaho:** Writing – review & editing, Data curation, Investigation, Formal analysis**,** **Budhy Kurniawan:** Investigation, Formal analysis, **Jan Setiawan:** Data curation, Investigation, Formal analysis, **Masno Ginting:** Writing – review & editing, Formal Analysis**, Andon Isnani:** Writing – review & editing, Formal Analysis, Validation, Supervision, **Januar Widakdo:** Writing – review & editing, Formal Analysis, Validation, Supervision.

REFERENCES

[1] Y. Zhang, *High-Entropy Materials-A Brief Introduction*, vol. 113, no. 9. 2019.

[2] K. Heriyanto *et al.*, "Neutron shielding performance of Cd/316L composite fabricated by arc plasma sintering," *Nucl. Mater. Energy*, vol. 40, no. July, p. 101718, 2024, doi: 10.1016/j.nme.2024.101718.

[3] M. K. Ajiriyanto, R. Kriswarini, Yanlinastuti, "Analisis korosi pipa pendingin sekunder rsg-gas dengan teknik electrochemical impedance spectroscopy," pp. 105–114, 2018.

[4] T. Firmansyah, B. Dilasari, J. Setiawan, and D. H. Prajitno, "Effect of Al, Zr and Mo on corrosion resistance of AlXCrFeNiMo and AlXCrFeNiZr (X=1, 1.2 and 1.4) as fuel cladding materials," *Urania J. Ilm. Daur Bahan Bakar Nukl.*, vol. 28, no. 1, p. 1, 2022, doi: 10.17146/urania.2022.28.1.6624.

[5] M. Hirano *et al.*, "Insights from review and analysis of the Fukushima Dai-ichi accident," *J. Nucl. Sci. Technol.*, vol. 49, no. 1, pp. 1–17, 2012, doi: 10.1080/18811248.2011.636538.

[6] M. Steinbrück, M. Große, L. Sepold, and J. Stuckert, "Synopsis and outcome of the QUENCH experimental program," *Nucl. Eng. Des.*, vol. 240, no. 7, pp. 1714–1727, 2010, doi: 10.1016/j.nucengdes.2010.03.021.

[7] Q. Wang, X. Kong, Y. Yu, T. Xin, and L. Wu, "Effect of B and Hf doping on vacancy defects in AlCrMoNbZr high entropy alloy: A first principles study," *J. Phys. Chem. Solids*, vol. 195, no. July, 2024, doi: 10.1016/j.jpcs.2024.112245.

[8] W. Zhang *et al.*, "Preparation, structure, and properties of high-entropy alloy multilayer coatings for nuclear fuel cladding: A case study of AlCrMoNbZr/(AlCrMoNbZr)N," *J. Nucl. Mater.*, vol. 512, pp. 15–24, 2018, doi: 10.1016/j.jnucmat.2018.10.001.

[9] E. Kashkarov *et al.*, "Recent advances in protective coatings for accident tolerant zr-based fuel claddings," *Coatings*, vol. 11, no. 5, pp. 1–32, 2021, doi: 10.3390/coatings11050557.

[10] W. Zhang *et al.*, "Interface stability, mechanical and corrosion properties of AlCrMoNbZr/(AlCrMoNbZr)N high-entropy alloy multilayer coatings under helium ion irradiation," *Appl. Surf. Sci.*, vol. 485, no. March, pp. 108–118, 2019, doi: 10.1016/j.apsusc.2019.04.192.

[11] M. K. Ajiriyanto, D. Anggraini, R. Kriswarini "Analisis korosi paduan ZIRLO-Mo dalam media NaCl menggunakan metode polarisasi," pp. 183–194, 2017.

[12] Z. Tao *et al.*, "Design and characterisation of AlCrFeCuNbx alloys for accident-tolerant fuel cladding," *J. Alloys Compd.*, vol. 859, no. 2, p. 157805, 2021, doi: 10.1016/j.jallcom.2020.157805.

[13] C. Xiang *et al.*, "Intermetallics Design of single-phase high-entropy alloys composed of low thermal neutron absorption cross-section elements for nuclear power plant application," vol. 104, no. October 2018, pp. 143–153, 2019, doi: 10.1016/j.intermet.2018.11.001.

[14] J. Setiawan, B. Dilasari, and D. H. Prayitno, "Phase Formation Prediction and Analysis of Multicomponent Alloys AlCrFeNiM (M = Mo and Zr)".

[15] B. J. Yeh *et al.*, "Nanostructured high-entropy alloys with multiple principal elements : novel alloy design concepts and outcomes," no. 5, pp. 299–303, 2004, doi: 10.1002/adem.200300567.

[16] Y. Zhang *et al.*, "Progress in materials science microstructures and properties of high-entropy alloys," *Prog. Mater. Sci.*, vol. 61, no. October 2013, pp. 1–93, 2014, doi: 10.1016/j.pmatsci.2013.10.001.

[17] K. Wang, X. Liu, T. Liu, C. He, and J. Liu, "applied sciences Interdiffusion in Zr-Mo /W Intermetallics," pp. 1–12, 2023.

[18] R. Salam, N. Shabrina, "Studi oksidasi paduan baja Fe-Cr-ZrO2 dengan metode sintesis high energy milling dan ultrasonic menggunakan thermogravimetri," pp. 51–57, 2021.

[19] H. Jin, X. Zhang, Y. Ding, S. He, Z. Lv, and F. Zhang, "Enhanced mechanical properties and corrosion resistance of $CrSiN/Al_2O_3$ multilayer films deposited by magnetron sputtering," *J. Mater. Sci.*, vol. 60, no. 7, pp. 3504–3517, 2025, doi: 10.1007/s10853-025-10667-2.

[20] Z. Shi, M. Liu, and A. Atrens, "Measurement of the corrosion rate of magnesium alloys using Tafel extrapolation," *Corros. Sci.*, vol. 52, no. 2, pp. 579–588, 2010, doi: 10.1016/j.corsci.2009.10.016.